Optics Communications 458 (2020) 124823

Contents lists available at ScienceDirect

Optics Communications

journal homepage: www.elsevier.com/locate/optcom

Intracavity generated visible self-reconstructing Bessel-like laser beams by thermal effect

Shengwei Cui [a], Bin Xu [a], Saiyu Luo [a], Huiying Xu [a], Zhiping Cai [a,*], Jixiong Pu [b], Sabino Chávez-Cerda [c]

[a] Department of Electronic Engineering, Xiamen University, Xiamen 361005, China
[b] Fujian Provincial Key Laboratory of Light Propagation and Transformation, College of Information Science & Engineering, Huaqiao University, Xiamen, Fujian 361021, China
[c] Instituto Nacional de Astrofísica, Óptica y Electrónica, Departamento de Óptica, Calle Luis Enrique Erro 1, Tonantzintla, Puebla Apdo. Postal, Mexico

ARTICLE INFO

Keywords:
Pr^{3+}-doped
Bessel-like beam
Solid-state laser

ABSTRACT

In this paper we report the intracavity realization of visible reconstructing Bessel-like beams when a thin Nd:YVO_4 crystal is inserted in a diode-pumped Pr:YLF laser at 639.5 nm. The position of the thin crystal and the intracavity power determine the Bessel-like mode generated. The self-reconstructing characteristic of the obtained Bessel-like beam is also demonstrated.

1. Introduction

Since the pioneering works of Durnin et al. in 1987 [1,2], Bessel beams have motivated considerable attention due to their fascinating properties of non-diffraction and self-reconstruction. Based on these properties, various applications have been reported for the Bessel beams. For example, Bessel beam has been used in interboard optical data distribution [3], 3D imaging [4], channeling radiation [5], microscopy and optical trapping [6–8]. Researches have shown that it not only reduces scattering effects, but also simultaneously increases image quality and penetration depth in dense media [7]. Good approximations to Bessel beams can be made in the laboratory and those with a Gaussian envelope are of common use [9,10]. Nevertheless, all of non-diffracting beams (Bessel–Gaussian, Airy beams, etc.), since they are composed by the interference of tilted waves, they can only exist within a finite length. These beams can only be studied within this well-defined region of validity.

There are several ways to realize Bessel–Gaussian beams, which can be sorted roughly into passive and active schemes [11]. The first category uses a passive optical element to convert an incoming laser beam to Bessel beams; such as an axicon, which is the most widely used approach, phase hologram, and Bessel beam kinoform [12,13]. The second category is formed by methods relying on a resonator frame to produce the Bessel beams [14–17]. This active system precludes the need for external optical elements and results in high output power and quality of the generated beam. Nevertheless, all of non-diffracting beams (Bessel–Gaussian, Airy beams, etc.), since they are composed by the interference of tilted waves, they can only exist within a finite length. These beams can only be studied within this well-defined region of validity.

Recent years, Bessel-like beams are presented as longitudinally dependent Bessel beams [18–21]. Bessel-like beams extended propagation distances as compared to conventional Bessel–Gaussian beams, with a far field pattern that is also Bessel–Gaussian in structure. However, recent studies have shown that Bessel-like laser beams are not solutions to the eigenmode equations of laser resonators with spherical curvature mirrors, and thus cannot be achieved (at least not as a single mode) from conventional resonator designs [21]. Until now, there are no experiment researches about intracavity Bessel-like beams.

On the other hand, coherent light sources emitting in the visible spectral have been studied for biomedical applications such as subdiffraction-resolution fluorescence imaging and laser-mediated photodynamic therapy [22,23]. Moreover, it is well known that trivalent praseodymium (Pr^{3+}) is capable of generating various laser emissions in visible band [24,25]. Therefore, in this letter, we demonstrate an experimental realization of Bessel-like beams in visible region based on a diode-end-pumped Pr:YLF intracavity laser system with the aid of a thin Nd:YVO_4 crystal.

2. Experimental setup

The schematic setup is shown in Fig. 1. A blue laser diode (LD) is used as a pumping source, and the central wavelength of the LD is 444 nm at maximum output power. The input mirror M1 is flat with high transmission of about 95% at around 444 nm and high reflectivity of 99.9% at 639.5 nm. Two output mirrors (M2) are used in this

* Corresponding author.
E-mail address: zpcai@xmu.edu.cn (Z. Cai).

https://doi.org/10.1016/j.optcom.2019.124823
Received 1 August 2019; Received in revised form 27 September 2019; Accepted 23 October 2019
Available online 28 October 2019

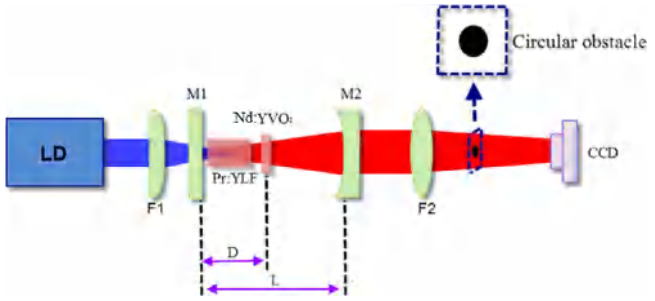

Fig. 1. Experimental setup for generating Bessel-like beams. F1 is a plano-convex lens. F2 is a biconvex lens. The distance D≈20 mm and cavity length L≈55 mm.

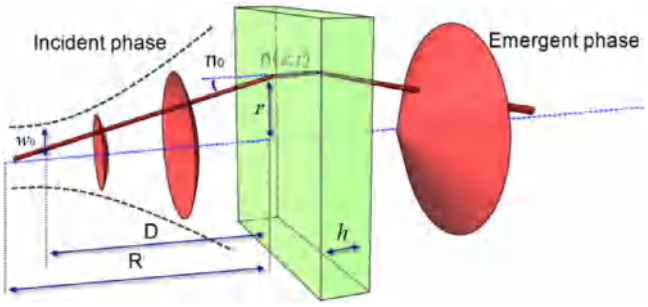

Fig. 2. Diagram of light beam passing through the Nd:YVO_4 crystal. n_0, n(z, r) are refractive indexes of air and crystal, respectively. h is the thickness of the crystal.

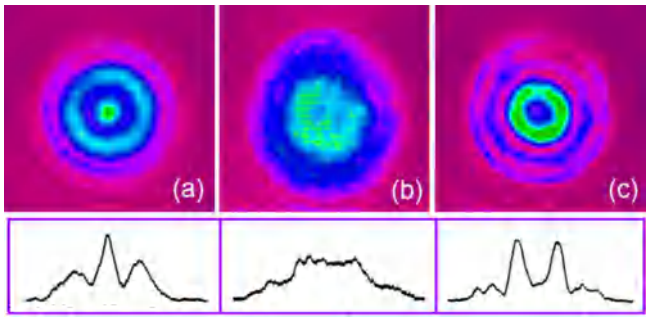

Fig. 3. Output laser beams with tuning the Nd:YVO_4 crystal at different positions. (a)–(c) Output laser beams from the perfect position of the Nd:YVO_4 crystal for Bessel-like beam to further distances.

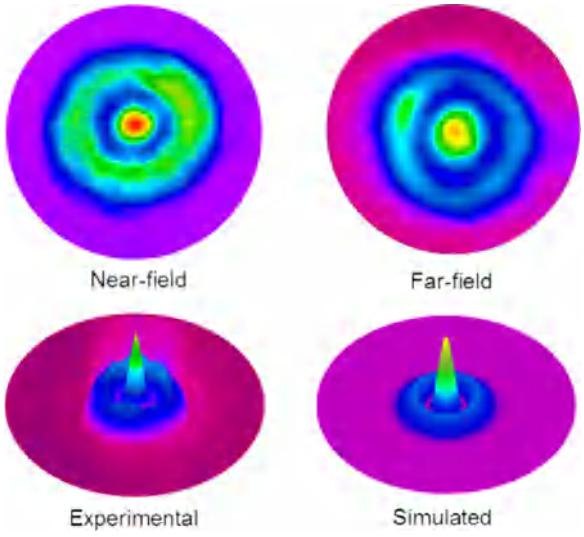

Fig. 4. Intensity distributions of output Bessel-like beam.

experiment with the same radii of curvatures of 50 mm and different transmissions as 1.8% and 3.2% at 639.5 nm. The laser gain medium is a 0.2at.% doped Pr:YLF crystal cut in a crystalline axis with dimensions as 3 × 3 × 8 mm^3 (8 mm in thickness). The Pr:YLF gain medium was wrapped inside indium foil and mounted in a water-cooled copper holder maintained at a temperature of 20 °C. In addition, a 1-mm-thin Nd:YVO_4 crystal cut in c crystalline axis is inserted between the Pr:YLF and output coupler. The role of the Nd:YVO_4 plate is to generate Bessel-like beam by introducing a gradient-index by the thermal effect. A convex lens and a circular obstacle are used to verify the self-reconstruction of Bessel-like beam. The intensity of output beam can be directly observed by a conventional charge-coupled device (CCD).

3. Analyzation and results

3.1. Analyzation

As shown in Fig. 2, a generalized Gaussian beam propagate through the thin Nd:YVO_4 crystal along the direction of z-axis. Assuming that the beam-waist position is taken at the origin of the coordinate system, the complex amplitude of the light field at the entrance plane of the Nd:YVO_4 can be written as [26–29]

$$E\left(r, z_0\right) = E\left(0, z_0\right)\exp(-\frac{r^2}{w_p^2})\exp(-\frac{ik_0 n_0 r^2}{2R}), \tag{1}$$

where r is the radial coordinate, z_0 is the position coordinate of the Nd:YVO_4 entrance plane from the initial plane (beam-waist), k_0 is the free-space wavenumber, n_0 is the refractive index of the air around the Nd:YVO_4, $n_0 = 1$. The beam radius at the Nd:YVO_4 entrance plane w_p and the wavefront curvature R of Gaussian beam can be expressed as

$$w_p(z) = w_0\sqrt{1 + \left(z/z_R\right)^2}, \tag{2}$$

$$R(z) = z\left[1 + \left(z_R/z\right)^2\right], \tag{3}$$

where w_0 is the Gaussian waist radius, and $z_R = \pi {w_0}^2/\lambda$ is the Rayleigh range.

After passing through the thin crystal, the total phase at the output plane of the Nd:YVO_4 can expressed as

$$\phi(r) = \frac{k_0 r^2}{2R} + \Delta\phi(r). \tag{4}$$

In this equation, the first term corresponds to the phase contribution of the beam curvature of the wavefront. The second term is the phase shift contribution related to the thermal effect of the thin crystal, which can be described as [30]

$$\Delta\phi(r) = \frac{2\pi}{\lambda}\int_0^h \left[\frac{\partial n}{\partial T}T(r) + \delta n\frac{\partial u(r)}{\partial z} + \sum_{i,j=1}^{3}\frac{\partial n}{\partial \epsilon_{ij}}\epsilon_{ij}(r)\right] dz, \tag{5}$$

where $\frac{\partial n}{\partial T}$ is the thermal dispersion, $\frac{\partial u(r)}{\partial z}$ is the relative axial elongation, and the last term represents the stain-induced birefringence with the strain tensor ϵ_{ij}. The result of the phase can be regarded as an aspherical focus lens.

Hence, after having propagated through the Nd:YVO_4, the complex electric field at the output of the Nd:YVO_4 will be

$$E\left(r, z_0 + h\right) = E\left(0, z_0\right)\exp(-\frac{r^2}{\omega_p^2})\exp(-\frac{\alpha T}{2})\exp\left[-i\phi(r)\right], \tag{6}$$

where α is the linear absorption coefficient of the thin Nd:YVO_4 crystal. The intracavitary thin crystal introduces a gradient-index by the thermal effect, which can be changed by adjusting the position in cavity.

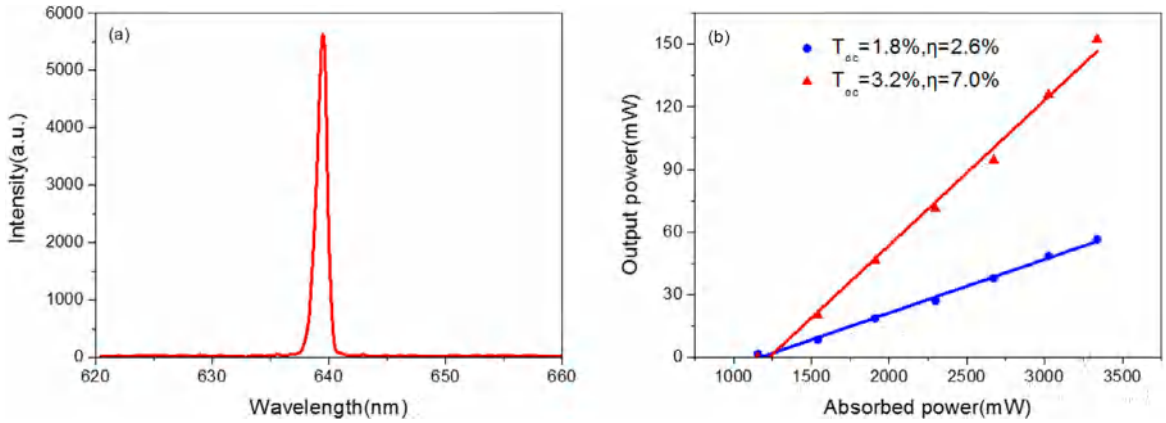

Fig. 5. (a) Spectrogram of output laser, (b) Input–output characteristics of diode-pumped Pr:YLF Bessel-like lasers at 639.5 nm for output coupler transmissions with 1.8% and 3.2%.

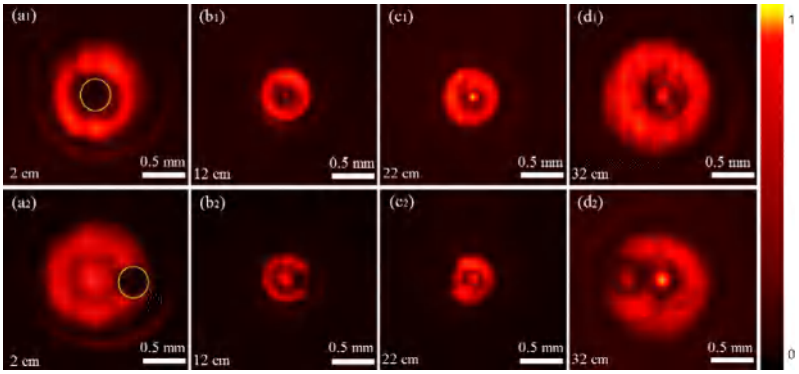

Fig. 6. Intensity distributions of Bessel-like laser beam after the circle obstacle: (a)–(d) the intensity distributions of different positions.

When the Nd:YVO_4 crystal was closed to the input mirror M1, where the beam radius is very small, and the modulated phase would be too large to get a stable Bessel-like laser. Fig. 3(a) shows the output Bessel-like laser beam with fine-tuning the Nd:YVO_4 crystal at the "perfect position" by using a micrometer adjuster. Otherwise, when increased the distance with the M1, the modulated phase would be smaller, and the central intensity of output laser beam will be decreased to be a flat-top Gaussian beam, shown in Fig. 3(b). Keep increasing the distance the output laser can be a donut-shape distribution, shown in Fig. 3(c). Moreover, from (a) to (c) the position of Nd:YVO_4 crystal only moved less than 3 mm. Other crystals also can instead the Nd:YVO_4 crystal. Nevertheless, the "perfect position" is different for other materials, due to each optical thermal coefficient introducing individual gradient-index. That is why we employ hemispherical linear resonator, which always can easily find the "perfect position" of the crystal to achieve Bessel-like beams.

3.2. Experimental results and self-reconstructing

Fig. 4 shows the near field, far field and three-dimensional intensity distributions of the output beam. It has a high intensity spot in the center of light beam, dark and bright rings circumfuse the central spot alternately. Compared with the simulated radial profile, the experimental result shows a similar distribution of zero-order Bessel function. Different from Bessel–Gaussian beams, the far-field intensity of output beam is also zero-order Bessel function distribution. It means that Bessel-like beams have infinity propagation distances with zero-order Bessel intensity distributions. Meanwhile, Bessel-like beams lack the ability of non-diffraction.

Because of the gradient-index is decided by the energy density, the distance between the M1 and Nd:YVO_4 is the key to realize Bessel-like laser beams in the resonator. It should emphasize that it is necessary for the laser cavity to operate at the stability limit (cavity length L ≈ 55 mm) in order to eliminate fundamental Gaussian laser beam, because the Bessel-like laser beam and fundamental Gaussian laser beam both exist within stability condition (L < 55 mm). Hence, this work demonstrates that intracavity method can easily achieve a much high power for the thermal effect, meanwhile, the effect will increase by multiple round-trip modulations. Moreover, by operating the loss of other modes in laser resonator can get a pure laser mode output. It is apparent that this method presents an easier route to generate Bessel-like beams inside a laser resonator.

Fig. 5(a) shows the spectrogram of the output laser by using an Ocean-Optics HR2000 + optical spectrum analyzer with the resolution of 0.035 nm, and the peak wavelength is 639.5 nm and the FWHM is about 0.8 nm. Fig. 5(b) shows the Bessel-like laser output power as a function of the absorbed pumped power of the Pr:YLF crystal. Maximum output powers for the 1.8% and 3.2% output couplers are respectively measured to be 56.5 mW and 152.4 mW with corresponding slope efficiencies of 2.6% and 7.0%. Moreover, the Bessel-like laser threshold is above 1 W. It is obvious that this Bessel-like laser has a far higher threshold and lower slope efficiency than that obtained with Gaussian laser output [24,25]. During the experiment, we also found another interesting phenomenon that the threshold of the oscillating start process is higher than running process due to the thermal effect.

To demonstrate that our achieved Bessel-like laser beams also have the property of self-reconstructing as Bessel–Gaussian beams [9,10], a circular obstacle with diameter of about 300 μm was used to block a part of the output beam. Fig. 6 shows the intensity distributions of different positions after the circle obstacle. The obstacle was placed on-axis in Fig. 6(a1)–(d1) and off-axis in Fig. 6(a2)–(d2). We moved the position of CCD to measure the intensity distributions of the beam in different

positions, (a)–(d) are 2 cm 12 cm 22 cm and 32 cm after the obstacle, respectively. It is easy to observe that, in a short transmission distance after the obstacle, the intensity of the blocked spot was dark. However, with the increasing of the distance, the dark spot became brighter. After a certain distance, the intensity distribution of the laser beam could reconstruct to be Bessel distribution again. Notice that when the obstacle is placed off-axis, its shadow appears diametrically opposite to its original position. This is a feature of the conic phase creating Bessel-like beam. The experimental results show that Bessel-like laser beams have a good self-reconstructing characteristic.

4. Conclusion

In conclusion, based on a diode-pumped Pr:YLF laser with hemispherical linear resonator, we realized Bessel-like laser beams in visible spectral region by inserting a thin Nd:YVO_4 crystal inside the laser cavity to introduce a gradient-index. The maximum output power of the red Bessel-like laser was up to more than 150 mW. Bessel-like beams have the intensity distributions of zero-order Bessel function both in near field and far field. The infinity propagation distances of Bessel-like beam is most different from Bessel–Gaussian beam. In addition, the property of self-reconstructing of the Bessel-like laser beam is also verified after a circular obstacle. Note that other kinds of Bessel-like lasers also can be obtained by this approach. This method for generating Bessel-like beams may have applications in laser processing and optical manipulation.

Funding

This work was supported by National Natural Science Foundation of China (NSFC) (11674269); Natural Science Foundation of Fujian Province of China (2018J01108); Principal fund of Xiamen University, China (20720180082); The International Collaborative Laboratory of 2D Materials for Optoelectronics Science and Technology, Shenzhen University, China (2DMOST2018026); The Scientific Research Foundation for Returned Scholars, Ministry of Education of China.

References

[1] J. Durnin, J. Miceli Jr, J. Eberly, Diffraction-free beams, Phys. Rev. Lett. 58 (1987) 1499.
[2] J. Durnin, Exact solutions for nondiffracting beams. I. The scalar theory, J. Opt. Soc. Amer. A 4 (1987) 651–654.
[3] R. MacDonald, S. Boothroyd, T. Okamoto, J. Chrostowski, B. Syrett, Interboard optical data distribution by Bessel beam shadowing, Opt. Commun. 122 (1996) 169–177.
[4] P. Zhang, M. Phipps, P. Goodwin, J. Werner, Confocal line scanning of a Bessel beam for fast 3D imaging, Opt. Lett. 39 (2014) 3682–3685.
[5] L. Schächter, W. Kimura, Vacuum channeling radiation by relativistic electrons in a transverse field of a laser-based Bessel beam, Phys. Rev. Lett. 114 (2015) 195501.
[6] D. McGloin, V. Garcés-Chávez, K. Dholakia, Interfering Bessel beams for optical micromanipulation, Opt. Lett. 28 (2003) 657–659.
[7] F.O. Fahrbach, P. Simon, A. Rohrbach, Microscopy with self-reconstructing beams, Nat. Photonics 4 (2010) 780–785.
[8] V. Garces-Chavez, D. McGloin, H. Melville, W. Sibbett, K. Dholakia, Simultaneous micromanipulation in multiple planes using a self-reconstructing light beam, Nature 419 (2002) 145–147.
[9] R. Piestun, J. Shamir, Generalized propagation-invariant wave fields, J. Opt. Soc. Amer. A 15 (1998) 3039–3044.
[10] J.C. Gutiérrez-Vega, M. Iturbe-Castillo, S. Chávez-Cerda, Alternative formulation for invariant optical fields: Mathieu beams, Opt. Lett. 25 (2000) 1493–1495.
[11] D. McGloin, K. Dholakia, Bessel beam: diffraction in a new light, Contemp. Phys. 46 (2005) 15–28.
[12] J.H. McLeod, The axicon: a new type of optical element, JOSA 44 (1954) 592–897.
[13] J. Turunen, A. Vasara, A.T. Friberg, Holographic generation of diffraction-free beams, Appl. Opt. 27 (1988) 3959–3962.
[14] A.N. Khilo, E.G. Katranji, A.A. Ryzhevich, Axicon-based bessel resonator: analytical description and experiment, J. Opt. Soc. Amer. A 18 (2001) 1986–1992.
[15] F. Wu, Y. Chen, D. Guo, Nanosecond pulsed Bessel-Gauss beam generated directly from a Nd:YAG axicon-based resonator, Appl. Opt. 46 (2007) 4943–4947.
[16] A. Hakola, T. Hakkarainen, R. Tommila, T. Kajava, Energetic Bessel-Gauss pulses from diode-pumped solid-state lasers, J. Opt. Soc. Amer. B 27 (2010) 2342–2349.
[17] S. Vyas, Y. Kozawa, S. Sato, Generation of radilally polarized Bessel-Gaussian beams from c-cut Nd:YVO_4 laser, Opt. Lett. 39 (2014) 1101–1104.
[18] Z. Jaroszewicz, J. Morales, Lens axicons: systems composed of a diverging aberrated lens and a perfect converging lens, J. Opt. Soc. Amer. A 15 (1998) 2383–2390.
[19] A.V. Goncharov, A. Burvall, C. Dainty, Systematic design of an anastigmatic lens axicon, Appl. Opt. 46 (2007) 6076–6080.
[20] V. Belyi, A. Forbes, N. Kazak, N. Khilo, P. Ropot, Bessel–like beams with z–dependent cone angles, Opt. Express 18 (2010) 1966–1973.
[21] I.A. Litvin, N.A. Khilo, A. Forbes, V.N. Belyi, Intra–cavity generation of Bessel–like beams with longitudinally dependent cone angles, Opt. Express 18 (2010) 4701–4708.
[22] M.J.C.i.d. Alexiades-Armenakas, Laser-mediated photodynamic therapy, Clin. Dermatol. 24 (2006) 16–25.
[23] M. Heilemann, S. Van De Linde, M. Schüttpelz, R. Kasper, B. Seefeldt, A. Mukherjee, P. Tinnefeld, M.J.A.C.I.E. Sauer, Subdiffraction-resolution fluorescence imaging with conventional fluorescent probes, Angew. Chem. Int. Ed. 47 (2008) 6172–6176.
[24] F. Starecki, W. Bolaños, A. Braud, J.-L. Doualan, G. Brasse, A. Benayad, V. Nazabal, B. Xu, R. Moncorgé, P. Camy, Red and orange Pr^{3+}: $LiYF_4$ planar waveguide laser, Opt. Lett. 38 (2013) 455–457.
[25] B. Xu, F. Starecki, D. Paboeuf, P. Camy, J.L. Doualan, Z.P. Cai, A. Braud, R. Moncorgé, Ph. Goldner, F. Bretenaker, Red and orange laser operation of Pr:KYF_4 pumped by a Nd:YAG/LBO laser at 469.1 nm and a ingan laser diode at 444 nm, Opt. Express 21 (5) (2013) 5567–5574.
[26] S.C. Cerda, J.M. Hickmann, Spatial instabilities in the propagation of a cylindrical beam in a Kerr medium, Opt. Commun. 156 (1998) 347–349.
[27] L. Deng, K. He, T. Zhou, C. Li, Formation and evolution of far-field diffraction patterns of divergent and convergent Gaussian beams passing through self-focusing and self-defocusing media, J. Opt. A: Pure Appl. Opt. 7 (2005) 409.
[28] C.M. Nascimento, M.A. Alencar, S. Chávez-Cerda, M.G. da Silva, M.R. Meneghetti, J.M. Hickmann, Experimental demonstration of novel effects on the far-field diffraction patterns of a Gaussian beam in a Kerr medium, J. Opt. A: Pure Appl. Opt. 8 (2006) 947.
[29] A.B. Villafranca, K. Saravanamuttu, Diffraction rings due to spatial self-phase modulation in a photopolymerizable medium, J. Opt. A: Pure Appl. Opt. 11 (2009) 125202.
[30] C. Pfistner, R. Weber, H.P. Weber, S. Merazzi, R. Gruber, Thermal beam distortions in end-pumped nd:yag, nd:gsgg, and nd:ylf rods, IEEE J. Quantum Electron. 30 (7) (1994) 1605–1615.